

Bioinspiration & Biomimetics



PAPER

Stretch-and-release fabrication, testing and optimization of a flexible ceramic armor inspired from fish scales

RECEIVED
14 June 2016

REVISED
30 August 2016

ACCEPTED FOR PUBLICATION
31 August 2016

PUBLISHED
13 October 2016

Roberto Martini and Francois Barthelat

Department of Mechanical Engineering, McGill University, 817 Sherbrooke Street West, Montreal, QC H3A 2K6, Canada

E-mail: francois.barthelat@mcgill.ca

Keywords: bio-inspiration, armors, stretch and release method, puncture resistance, impact resistance

Supplementary material for this article is available [online](#)

Abstract

Protective systems that are simultaneously hard to puncture and compliant in flexion are desirable, but difficult to achieve because hard materials are usually stiff. However, we can overcome this conflicting design requirement by combining plates of a hard material with a softer substrate, and a strategy which is widely found in natural armors such as fish scales or osteoderms. Man-made segmented armors have a long history, but their systematic implementation in a modern and a protective system is still hampered by a limited understanding of the mechanics and the design of optimization guidelines, and by challenges in cost-efficient manufacturing. This study addresses these limitations with a flexible bioinspired armor based on overlapping ceramic scales. The fabrication combines laser engraving and a stretch-and-release method which allows for fine tuning of the size and overlap of the scales, and which is suitable for large scale fabrication. Compared to a continuous layer of uniform ceramic, our fish-scale like armor is not only more flexible, but it is also more resistant to puncture and more damage tolerant. The proposed armor is also about ten times more puncture resistant than soft elastomers, making it a very attractive alternative to traditional protective equipment.

1. Introduction

Over millions of years of evolution, animals have developed highly efficient protective systems to resist mechanical threats from predation, intraspecies fighting and hazardous environments [1]. Some of the most successful species in this evolutionary arms race combine high mobility with mechanical protection. Natural dermal armors have the flexibility to allow for unhindered movements, yet hard enough to resist punctures and lacerations. In nature, the conflicting requirement of hardness and compliance are resolved by covering a highly flexible membrane with hard plates of finite size, as shown in figure 1. The three natural dermal armors in figure 1 were taken from a distinct taxonomic family and species, but they share universal characteristics: (i) the scales are several orders of magnitude stiffer and harder than the softer skin and tissues that they protect; (ii) they form periodic scalation patterns over the whole surface of the skin; (iii) the size of the individual scales is about

one order of magnitude smaller than the overall size of the animal; (iv) the scales overlap in order to cover weak junctions, and in order to generate multilayered protections. Individual scales also have outstanding properties in terms of surface hardness, fracture toughness and overall resistance to sharp puncture [1–5]. The interactions between the scales govern local flexural behavior [6, 7], for example, by providing a compliant response at low bending curvature followed by stiffening at high curvatures [8]. The interaction between scales also improves puncture resistance by protecting the weak junctions between scales [7], and by adding mechanical stability [9].

Combining surface hardness with high flexural compliance is attractive for a variety of applications where flexible protection is needed; notably, scaled flexible protective armors have a long history. Lamellar armors made of hard plates laced together were used in ancient Egypt (17th century BC) [12]. The use of this type of armor spread across many different cultures, from applications in Assyrian to Mongolian

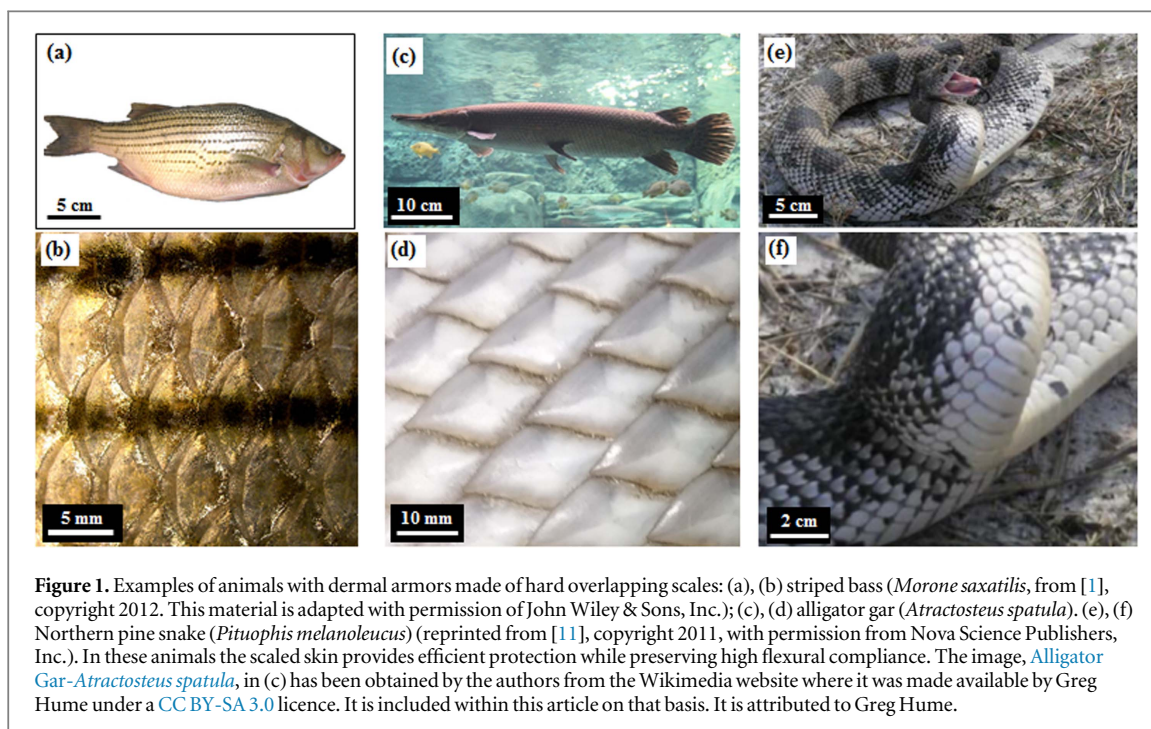
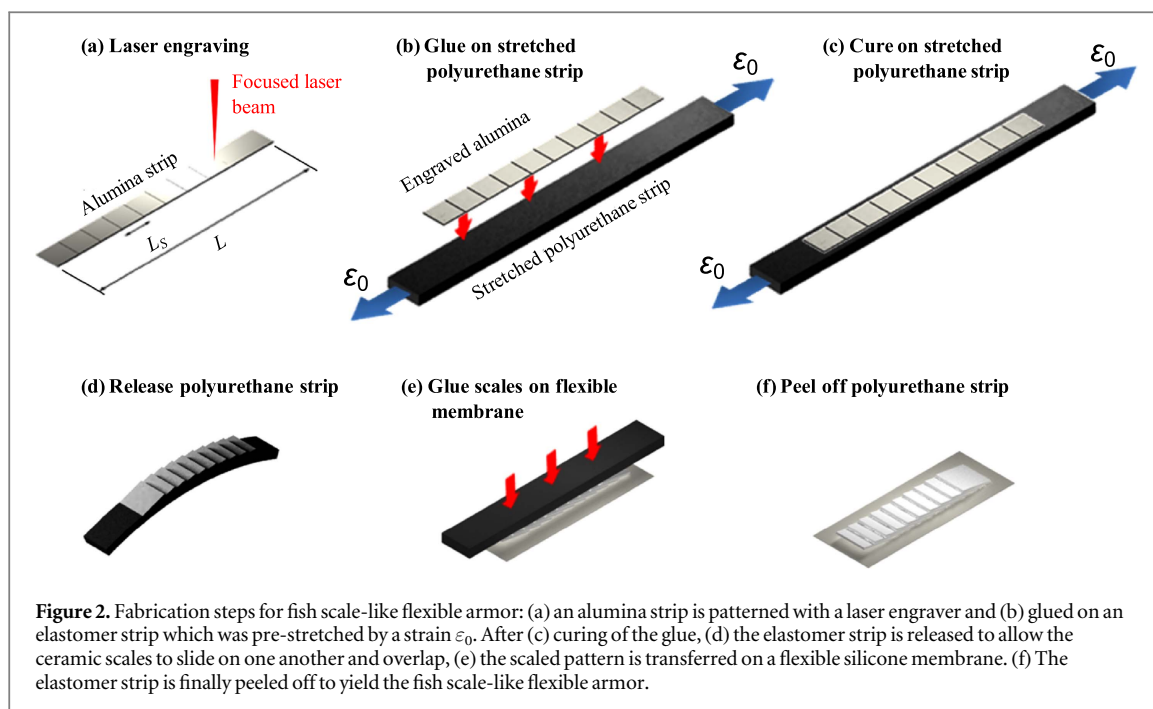


Figure 1. Examples of animals with dermal armors made of hard overlapping scales: (a), (b) striped bass (*Morone saxatilis*, from [1], copyright 2012. This material is adapted with permission of John Wiley & Sons, Inc.); (c), (d) alligator gar (*Atractosteus spatula*). (e), (f) Northern pine snake (*Pituophis melanoleucus*) (reprinted from [11], copyright 2011, with permission from Nova Science Publishers, Inc.). In these animals the scaled skin provides efficient protection while preserving high flexural compliance. The image, [Alligator Gar - *Atractosteus spatula*](#), in (c) has been obtained by the authors from the Wikimedia website where it was made available by Greg Hume under a [CC BY-SA 3.0](#) licence. It is included within this article on that basis. It is attributed to Greg Hume.

militaries [12]. Similar structures that are also spread across history are the scale armors, which instead consists of hard plates sewn on a backing fabric [12]. A typical example is the Roman Lorica squamata, which was made of small iron or bronze plates sewn onto fabric in a staggered fashion, similar to fish scales [13]. The same design is found in the gyorin kozane [14], a Japanese armor of the 11th century AD. This design later evolved into the medieval and then modern mail armor, where metallic rings are meshed together to form a flexible and protective armor. Mail armors provide protection upon blunt puncture while also providing good mobility, but they offer little resistance from sharp punctures with sharp objects which may penetrate between the rings. Mail armor is still used in modern butcher gloves and shark proof suits. Most of the flexible protective systems used today are based on advanced textiles of aramid (e.g. Kevlar®) or polyethylene (Spectra®) fibers [15, 16]. A typical stab resistant system used for industrial protection is several millimeters thick and it is composed of knitted aramid fabric impregnated with thermoplastic polymers [17]. These materials offer good general protection against cuts [18], but sharp and slender objects can easily penetrate between the threads of the fabric [19]. The impregnation of the fabric with thermoplastic polymers [19] or shear thickening fluids [20] increases the puncture resistance of the fabric by keeping the bundles of fiber together and thus reducing the ‘windowing’ of the fabric [17], at the expense of flexibility [21]. Other examples of modern flexible body armors incorporate hard elements, for example the ‘Dragon skin armor’ [22] is made of overlapping ceramic disks which provide some ballistic protection but at the

expense of mobility. Research groups have recently proposed alternative pathways to design and fabricate flexible armors using natural dermal armor as inspiration. Chintapalli *et al* [23] fabricated flexible armors inspired by armadillo osteoderms, consisting of hexagonal glass plates (manufactured by laser engraving) on a rubber substrate. The design presented an improved resistance upon puncture at the center of the scales but the design has weaknesses at the junction between the scales [23] and also due to tablet instability [9]. Ghosh *et al* [24] used 3D printed acrylonitrile butadiene styrene (ABS) scales glued on a thick vinyl polysiloxane elastomer to study the kinematics of scaled structures. Rudykh *et al* [7] proposed a structure of 3D printed scales with an ABS-like photopolymer on an elastomeric material, and used this material to analyze the effects of the volume concentration and angle of the scales on the bending and penetration stiffnesses. Funk *et al* [25] fabricated an armor that mimicked the structure of the teleost fish by sewing cellulose acetate butyrate (CAB) on a polypropylene mesh by means of a cotton thread. Although these structures duplicate many of the morphological features observed on fish skin, they are made of polymers which lack the hardness required for high-performance protection. In this work, we develop a systematic ‘transfer of technology’ from nature to engineer flexible armors. We propose a new method to manufacture synthetic dermal armor inspired by fish skin inspired by the controlled buckling method used to fabricate flexible electronics [26–28]. The method consists in bonding a pre-patterned ceramic material on a pre-strained elastomer strip, followed by the release of the strains to overlap individual scales in a



staggered overlapped fashion similar to fish scales. The scaled structure was then transferred onto a flexible backing substrate, the system was then tested against flexion and sharp puncture methods. The objectives of this bioinspired protective material were to (i) duplicate the very high contrast of properties between the scales and the substrate; (ii) generate overlapping pattern of scales using a scalable and easy method; (iii) characterize the resistance to sharp puncture and the flexural compliance for this protective system.

2. Fabrication

In order to duplicate the large contrast of properties observed in natural armor, we used high purity alumina for the scales (Young's modulus = 300 GPa) and a soft silicone elastomer for the membrane (Young's modulus = 10 MPa). We chose a thickness of 0.6 mm for the ceramic plates used in this work, which offered a good combination of protection and which could be easily processed and handled. The fabrication steps are shown in figure 2. The protocol started by cutting the plate into 5 mm wide strips and 115 mm long. The strip was then patterned with parallel trenches, about 100 μm deep using a laser-engraver (Model Vitrolux, Vitro Laser Solutions, Germany), equipped with a pulsed UV laser (power = 200 mW, wavelength = 355 nm). The depth of the trench was chosen to 'score' the surface of the ceramic and to ensure that individual scales could fracture and detach along the trenches. The trenches were carved at a distance L_s apart (figure 2(a)), which defined the final length of the synthetic ceramic scales. Systems with scale size of $L_s = 2.5$ mm, 5 mm, 7 mm and 10 mm were fabricated. Meanwhile, a strip of pre-

stretched polyurethane (width = 30 mm, thickness = 3 mm) was prepared by clamping the ends of the strip onto a miniature vice, and by stretching the strip to a desired strain (measured using marks on the strip). Pre-stretch strains of $\epsilon_0 = 0.25$, 0.5, 0.75 and 1 were used. The patterned alumina strip was then bonded on the surface of the pre-stretched polyurethane strip using a cyanoacrylate adhesive (figure 2(b)) which was allowed to completely cure for about ten minutes (figure 2(c)).

Individual scales were then separated by fracturing the strip along the laser-engraved trenches, which was facilitated by applying small, localized bending moments. Once the alumina scales were fully separated, the tensile strain in the polyurethane strip was slowly released (figure 2(d)) and in this process the stiff scales gradually overlapped, forming a scalation pattern similar to fish scales. In this process, the trailing edge of each scale acted as a wedge which partially debonded the neighboring scale from the substrate. The released strip displayed some residual bending from incomplete release of pre-strains in the substrate; however, these residual deformations were removed in the next fabrication step. A flat, stress-free 300 μm thick backing membrane made of silicone was coated with a 1 mm film of silicone adhesive using a doctor-blading method. The scaled alumina-polyurethane strip was pressed on the substrate using a vice which forced the strip into a straight shape and which infiltrated the interstices and gaps between the scales with silicone (figure 2(e)). After curing of the silicone adhesive for 12 h, the elastomer strip was peeled off the alumina scales to obtain the final material, consisting of ceramic scales bonded on a flexible membrane shown on figure 2(f). The successful transfer of the scales from the polyurethane strip onto the silicone

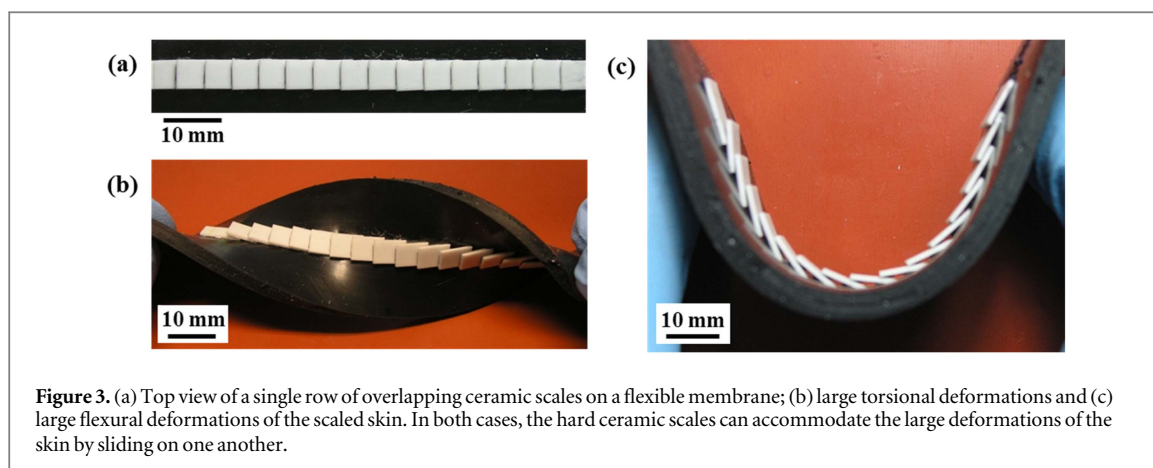


Figure 3. (a) Top view of a single row of overlapping ceramic scales on a flexible membrane; (b) large torsional deformations and (c) large flexural deformations of the scaled skin. In both cases, the hard ceramic scales can accommodate the large deformations of the skin by sliding on one another.

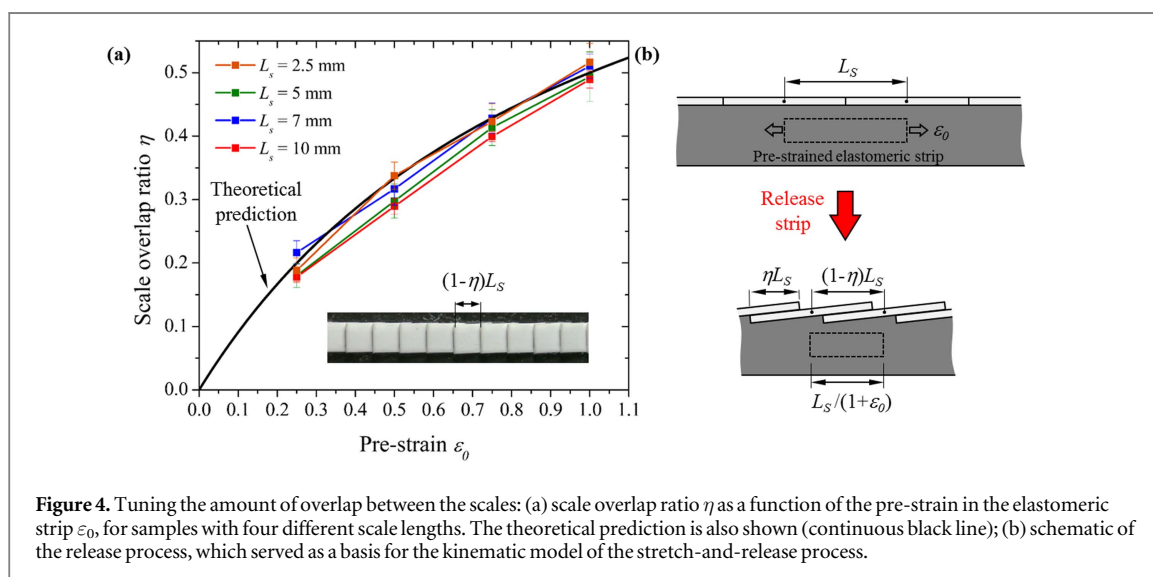


Figure 4. Tuning the amount of overlap between the scales: (a) scale overlap ratio η as a function of the pre-strain in the elastomeric strip ϵ_0 , for samples with four different scale lengths. The theoretical prediction is also shown (continuous black line); (b) schematic of the release process, which served as a basis for the kinematic model of the stretch-and-release process.

membrane relied on a careful choice of adhesives. The adhesion of the alumina scales on the polyurethane strip (provided by cyanoacrylate) was weaker than the adhesion of the alumina scales on the silicone backing membrane (provided by the silicone adhesive). Figure 3 shows the obtained scalation pattern on a soft polyurethane membrane. The fabrication method produced a regular scalation pattern, with no residual deformation. The ceramic scales provided a very hard surface, yet the skin could be easily twisted or bent (figure 3).

We examined the effect of two critical design parameters on the mechanical performance of the scaled skin: the length of the individual scales L_s and their overlap η , which was defined as the ratio between the overlapping length and the length of the scale when the system was in the un-deformed, straight configuration. The length of the scales L_s was controlled by changing the spacing between the engraved lines on the initial ceramic strip (figure 2(a)), and the overlap between the scales was controlled by simply adjusting the pre-stretch ϵ_0 in the polyurethane strip (figure 2(b)). Figure 4(a) shows the overlap ratio η measured on actual samples obtained using different

levels of pre-stretch ϵ_0 and for different scale sizes L_s . As expected, zero pre-stretch produces overlapped. Larger pre-stretches ϵ_0 lead to increased overlap between the scales, because the scales must accommodate more displacement toward each other as the strip is released. Fabrication tests using scales of different sizes showed that the size of the scales had little effect on the final overlap (figure 4(a)). In this work we generated scaled skin with up to about 50% overlap ($\eta = 0.5$) by applying a pre-strain $\epsilon_0 = 1$. Higher scale overlaps may be achieved by further increasing the pre-strain level.

These results indicate that the overlap between the scales can be accurately and reliably controlled by tuning the pre-strain in the polyurethane strip. A better understanding of the effect of the pre-strain in the release process can be gained from the simple kinematic model shown in figure 4(b). In this two-dimensional model, the initial configuration is an array of adjacent rigid scales which are perfectly bonded on a pre-stained and much softer elastic strip. Upon release of the tension in the strip, the displacement of the scales toward one another must match the release of strain in the strip (assuming that no residual

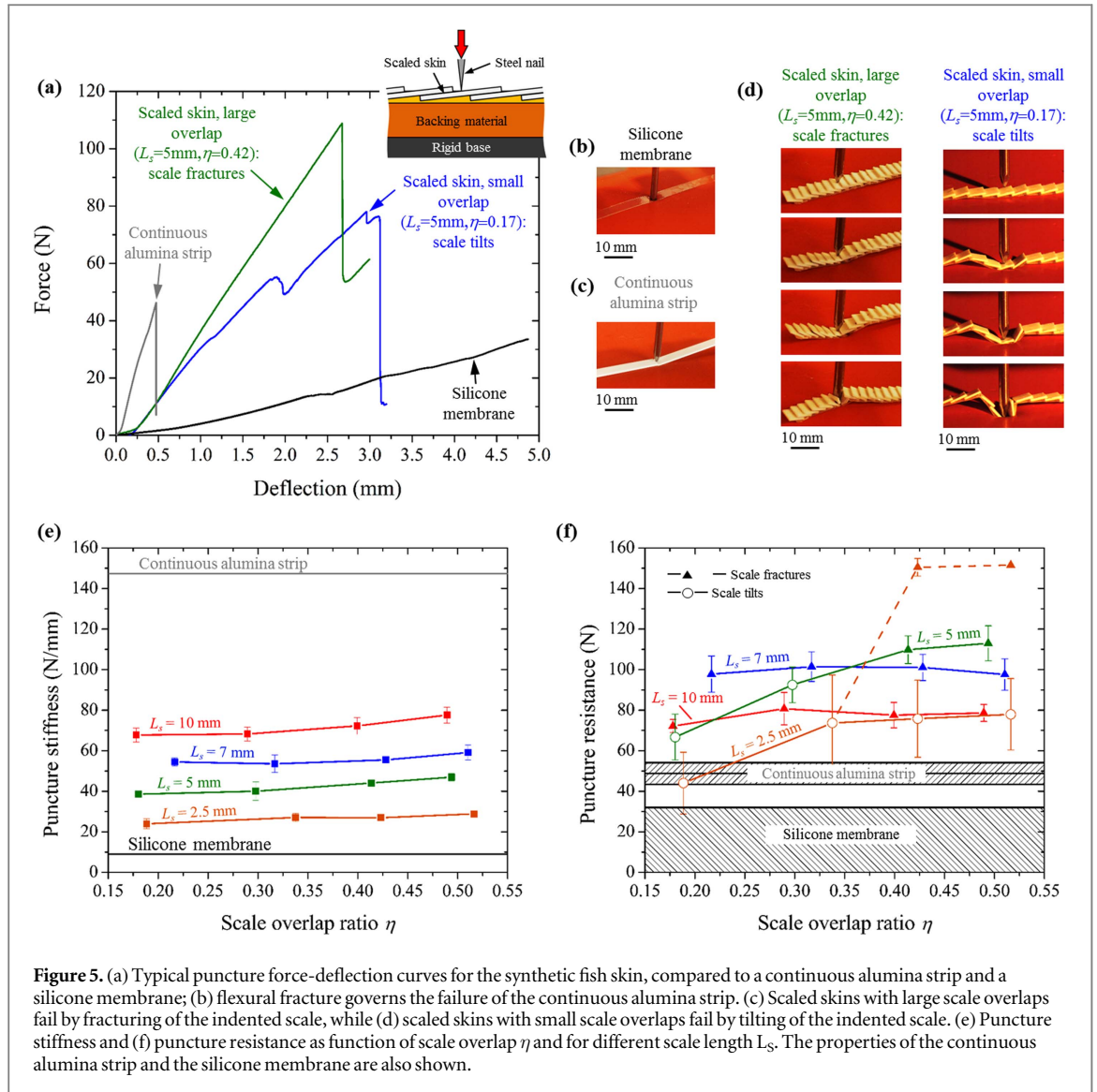


Figure 5. (a) Typical puncture force-deflection curves for the synthetic fish skin, compared to a continuous alumina strip and a silicone membrane; (b) flexural fracture governs the failure of the continuous alumina strip. (c) Scaled skins with large scale overlaps fail by fracturing of the indented scale, while (d) scaled skins with small scale overlaps fail by tilting of the indented scale. (e) Puncture stiffness and (f) puncture resistance as function of scale overlap η and for different scale length L_s . The properties of the continuous alumina strip and the silicone membrane are also shown.

deformation is left in the strip after full release), so that:

$$(1 - \eta)L_S = \frac{L_S}{1 + \varepsilon_0} \quad (1)$$

it follows that:

$$\eta = \frac{\varepsilon_0}{1 + \varepsilon_0}. \quad (2)$$

Figure 4(a) shows the prediction of this simple model together with the experimental results. The agreement of the model with the experiment is good, the experiment being slightly lower than the model most likely because some residual strains may still be trapped in the polyurethane strip after release. The model also confirms that the final overlap does not depend on the length of the scales. This simple model can therefore serve as a simple guideline to generate scaled pattern with a controlled amount of overlap.

3. Resistance to sharp puncture

We assessed the performance of the alumina scales against sharp punctures using a MTS testing machine (Eden Prairie, MN, USA) equipped with a 5 kN load cell at a crosshead rate of $50 \mu\text{m s}^{-1}$. The scaled skin was placed onto a block of soft backing material made of silicone rubber (Young's modulus $\sim 1 \text{ MPa}$) to simulate the compliant response of the soft tissues (dermis, muscles) underlying the flexible armor. A sharp steel nail with a diameter of 2 mm and a tip radius of 0.37 mm was mounted on the cross-head and driven into the scaled skin until the steel nail penetrated the skin. In order to assess the puncture resistance in the 'worst case' scenario, the scales were punctured on the weakest regions where the scaled skin was only one scale thick, which is where the least puncture resistance was expected. When we indented regions of the scaled membrane which were more than one scale thick, the resistance to puncture increased by about 40%, supplementary material, figure S1. Figure 5(a) shows typical force-deflection curves from

puncture experiments on scaled skins, continuous alumina strip and bare silicone membrane. Puncture tests on the silicone membrane shows large deflections, the needle pushing the membrane into the backing material. The test was interrupted once the membrane was punctured, even if the force kept increasing with displacement due to frictional forces between the sides of the nail and the backing material. The membrane tore progressively but at very high deflections and localized strains in the backing material (figure 5(b)). Soft tissues underneath such a soft membrane would accumulate blunt damage from excessive localized shearing even before the membrane is punctured. Thus, the membrane provides inadequate protection. In contrast, the puncture of a continuous alumina strip showed small and linear deformations because the stiff alumina strip distributes the force applied by the indenter over a large area on the soft backing material. The strip eventually failed in a brittle fashion and at a much higher force compared to the bare silicone membrane. Failure occurs by flexural stresses (figure 5(c)), which is typical of stiff films over soft substrates [29] (the exact shape of the tip of the nail has therefore little effect on the strength of the scales). The scaled skin displayed a puncture response with a stiffness intermediate between the silicon membrane and the continuous alumina strip (figure 5(a)). The indented scales redistributed the stresses of the indenter to some extent, preventing penetration of the nail into the backing material. Indentation was generally accompanied by deflection and to a degree, rotation of the scales neighboring the indented scales, which is dependent on the size and arrangement of the scales. In a way, this is similar to previous observations on 3D printed scaled skins [30]. Compared to the bare silicone membrane, the puncture stiffness of the scaled systems was 9 times higher, and the puncture resistance was up to 10 times higher. Compared to the continuum alumina layer, the puncture stiffness of the scaled system was 1.8 times lower, because the scales could deflect and tilt more easily. More unexpectedly, the puncture resistance of the scaled skin could be up to three times higher than the puncture resistance of the continuous alumina strip. The increase in puncture resistance by segmentation, recently captured on hexagonal glass plates on soft substrates [23], is explained by the reduction of the flexural span of smaller plates, which leads to lowered flexural stresses and which therefore delays fracture. It is therefore possible, using segmentation of hard plates, to simultaneously combine low puncture stiffness and high resistance to penetration. An implication of these experimental observations is that puncture stiffness should not be used as an indicator of puncture resistance, as previously suggested [7]. In our experiments the individual scales failed in one of two failure modes (figure 5(d)). For cases where the scales were large and with large overlaps, the indented scale

fractured from flexural stresses. In other cases, where the overlap was small, the indented scale tilted under the action of the indenter, providing a path for the indenter into the soft substrate, without fracturing the scale. This failure mode, recently documented with experiments and models, is highly detrimental and is translated into lower puncture resistance compared to the cases where the scale fractured [9].

The size and overlap of the scales clearly influence the performance and failure mode of the scaled skin under sharp punctures. In order to better understand and optimize this system, we fabricated and tested scaled skin with different combinations of L_S and η . Figure 5(e) shows the puncture stiffness for various combinations of these parameters. The results show that the scaled skin is always stiffer than the silicone membrane and more compliant than the continuous alumina strip. Larger scales produce stiffer responses, since large scales deform a larger volume of the backing material (this result is consistent with previous experiments [23]). The puncture stiffness also increased with larger scale overlaps η , which promoted the interaction of individual scales around the puncture site with the effect of distributing the puncture force over a greater area of the backing materials. This observation is consistent with previous observation on natural fish skin [31]. Figure 5(f) shows the puncture resistance of the scaled skins. All combinations of L_S and η explored here produced skins which were stronger than both the silicone membrane and the continuous alumina strip. Remarkably, the scaled skin was up to three times more resistant to punctures compared to the continuous alumina strip. When large scales were used ($L_S = 7$ mm and 10 mm), failure of the artificial fish skin always occurred by flexural fracture of the indented scale. $L_S = 7$ mm produced a higher puncture resistance, but the overlap had little effects on puncture resistance (figure 5(d)). A further decrease of L_S to 5 mm and 2.5 mm further increased the puncture resistance but only for large overlaps, smaller overlaps lead to a sharp drop in puncture resistance (figure 5(f)). As recently captured in models and experiments, smaller scales are more likely to tilt which leads to a significant drop in puncture resistance [9]. A strategy to delay tilting and improve stability is to use larger overlaps to promote contact interactions between neighboring scales. Our results show that small scales with $L_S = 5$ mm are stable only for $\eta > 0.4$. Most of the scales with $L_S = 2.5$ mm failed by tilting, except in a few experiments with $\eta > 0.4$ for which flexural fracture was achieved. These few cases produced the highest resistance to puncture achieved in the entire experimental set (figure 5(f)). In summary smaller scales can lead to much higher puncture resistance compared to continuous alumina, provided that tilting failure is delayed by promoting scale-scale interactions using large overlaps.

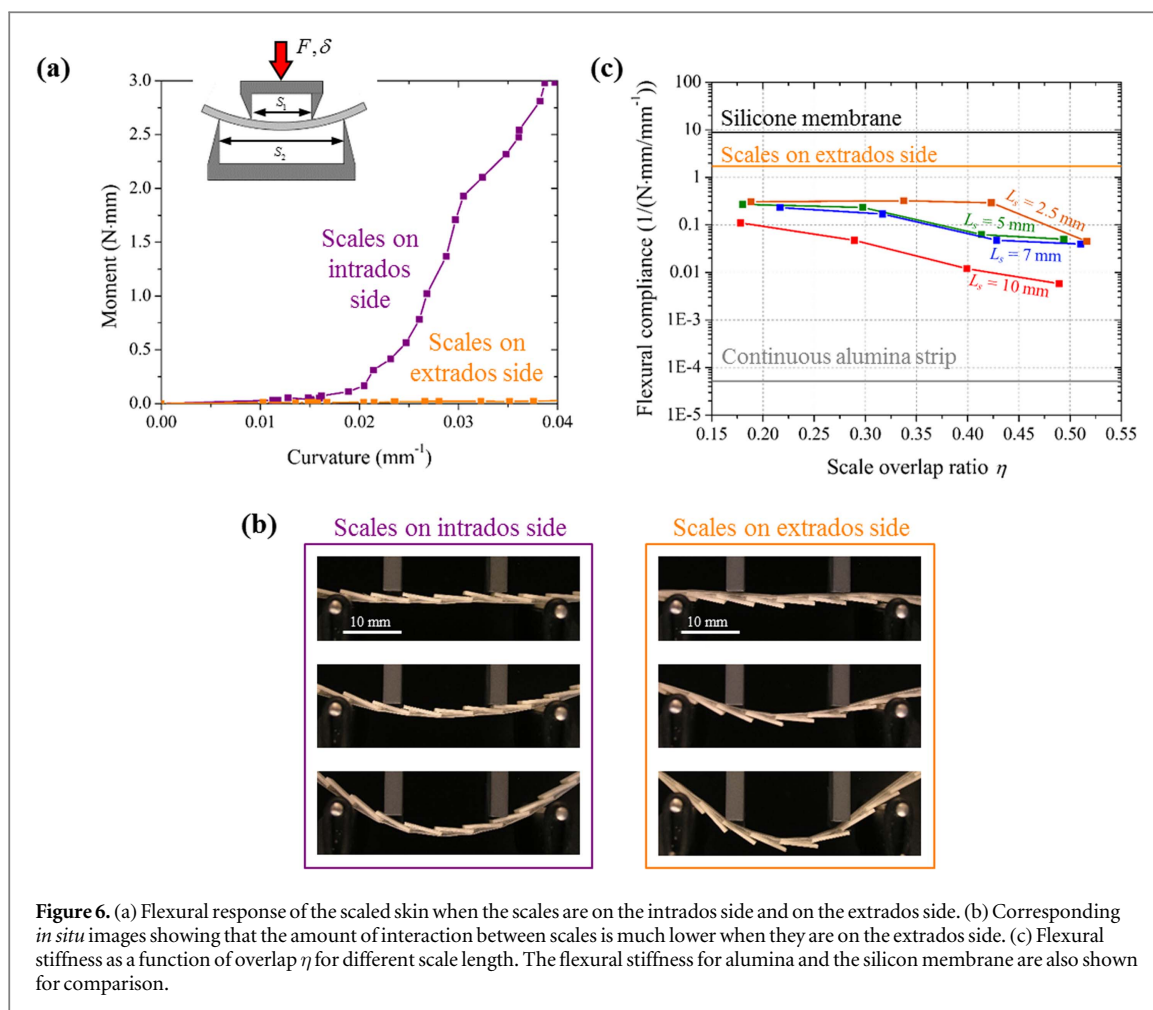


Figure 6. (a) Flexural response of the scaled skin when the scales are on the intrados side and on the extrados side. (b) Corresponding *in situ* images showing that the amount of interaction between scales is much lower when they are on the extrados side. (c) Flexural stiffness as a function of overlap η for different scale length. The flexural stiffness for alumina and the silicon membrane are also shown for comparison.

4. Flexural compliance

A high flexural compliance (or equivalently, a low flexural stiffness) is a desired property for a synthetic scaled skin to allow for unimpeded motions. Here we assessed the flexural response of strips of scaled skins identical to the ones used for the puncture tests. The samples were tested in a four-point bending configuration with an inner span $S_1 = 23 \text{ mm}$ and an outer span $S_2 = 36 \text{ mm}$, together with a miniature loading stage (ADMET Inc., Norwood, MA, USA) at a rate of $20 \mu\text{m/s}$. The advantage of the four-point bending configuration is that the bending moment M is uniform in the inner span section of the sample, and that it can be easily computed using $M = (F/4)(S_2 - S_1)$ where F is the force recorded by the load cell. As a result of the uniform bending moment in the inner span region, a uniform curvature of the sample is also expected. We verified this by fitting arc of circles onto pictures of the deformed sample acquired images during the test. This optical method was used to compute the radius of curvature R , from which we computed the curvature $C = 1/R$. The procedure was used to compute the bending moment-curvature curve for each of the samples (figure 6). The scaled membranes were tested in two possible

configurations: in the first configuration the scales were on the extrados side of the samples, corresponding to the ‘tensile’ side of the flexural sample. As expected this configuration was extremely compliant and offered little resistance to bending, because the scales moved apart and did not interact. The resulting flexural compliance in this configuration is similar to the bare silicone membrane (figure 6(b)). In the second flexural configuration, the scales were on the intrados side of the sample, on the compressive side. This configuration produced much stiffer responses, because the scales moved closer together and interacted through direct contact and friction (figure 5(b)) [6, 8]. The flexural response was non-linear with an initially soft response which stiffened as flexural deformations increased, as described in models previously developed for fish scales in bending [6, 8]. The curves also displayed multiple jumps, due to the scales shifting under the contact points of the four-point bending fixtures. Although the flexural response of the scaled skin is highly non-linear, we found that the initial bending stiffness reflects the overall stiffness of the scaled skin even during large deformation events. Therefore, we used the initial stiffness as a measure of the flexibility of the scaled skin.

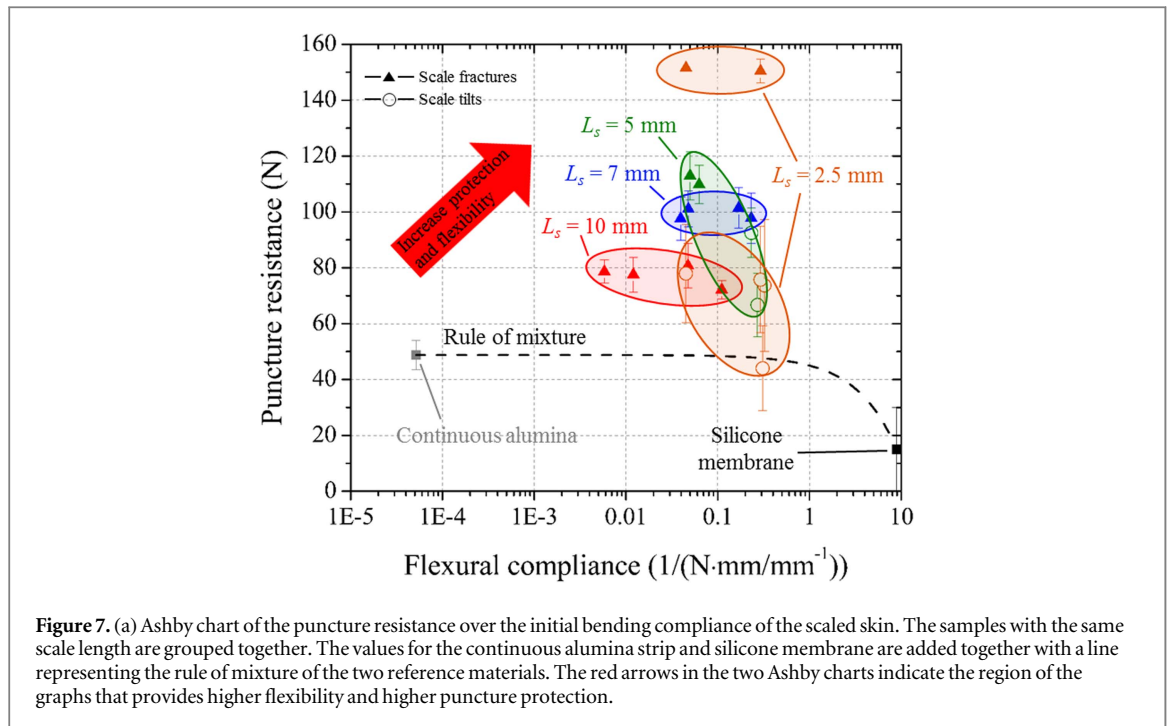


Figure 6(c) shows the flexural compliance of samples with different combinations of scale size L_s and scale overlap η . In the scale-on-extradors configuration, the scaled skin had a very high compliance comparable with the bare membrane, regardless of L_s and η . The scales-on-intradors configuration produced a much less compliant response, 2–4 orders of magnitude lower than the bare silicone membrane but also higher than the alumina strip by 2–4 orders of magnitudes. The results also show that the compliance decreases for larger scales, an effect which is even more pronounced for larger overlaps. Smaller scales produced more compliant system, with a smaller effect of overlap. When high flexural compliance is desired, smaller scales and smaller overlap should therefore be selected at the design stage.

5. Summary

The proposed stretch-and-release method is relatively easy to implement and can produce fish skin-like flexible membranes covered with hard ceramic plates, with highly controlled scale size and overlap. The puncture and flexural tests presented here give useful insight into the mechanics of this type of system, and it suggests optimization pathways to combine high resistance to puncture with flexural compliance. These two key attributes are plotted on an Ashby chart [32] on figure 7. The construction of scaled skins is often believed to be a compromise between resistance to puncture and flexibility [25]. Our results show that this is not the case, the scaled skins we tested have a much higher resistance to puncture than silicone, continuous alumina, as well as predictions from the rule of mixture based on these two materials. We also found

that smaller scales with a high overlap performed the best in terms of combined puncture resistance and compliance, provided that tilting of the scales can be prevented. Tilting of the scales is a highly detrimental failure mode which is inherent to hard plates on soft substrates [9]. The stability of the scales may however be improved by increasing the coefficient of friction of the surface of the scale [9], or by changing the geometry and arrangement of the scales in order to promote scale–scale interactions. Further experiments and models would be needed to optimize these parameters for specific applications. In the proposed material, the localization of the damage to a single scale suggests that the protective layer may retain the same resistance upon puncture after one scale has already failed. Experiments on damaged synthetic scaled skins showed that our scaled skin retains the full resistance upon multiple punctures, even when consecutive punctures are only two scales apart. The synthetic scaled skin is therefore damage tolerant with ‘multi-hits’ capabilities (supplementary material, figure S2).

The body of experiments provided in this article provides a strong basis for future design, optimization and fabrication of bio-inspired ceramic-based flexible armor. When properly designed, these systems can lead to remarkable combinations of compliance and resistance to penetration for a variety of protective applications. In this work we have opted for a structure of rectangular alumina scales on a flexible silicone membrane but, provided that the right adhesives are employed, the technique can be easily generalized to other materials or scales with other thicknesses or geometries. In our experiments, for instance, we were able to obtain similar structures by bonding glass scales on

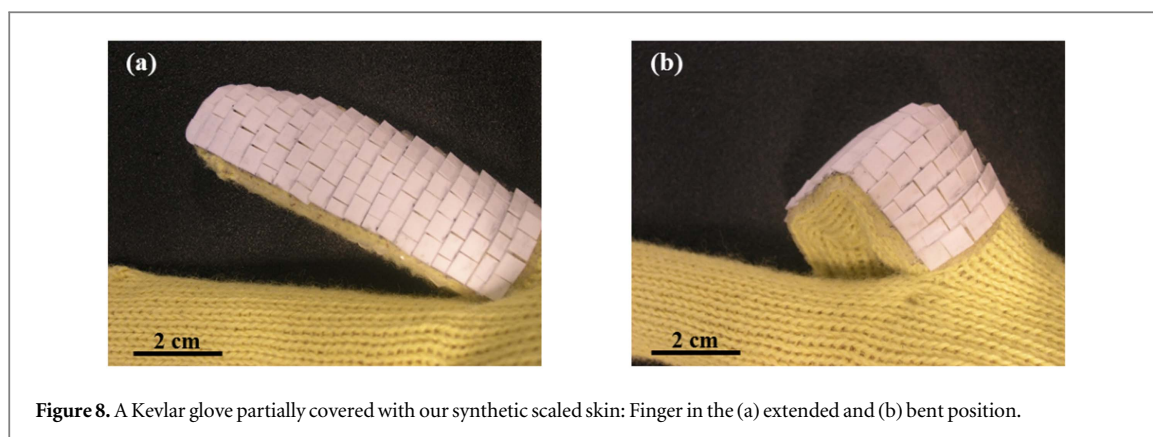


Figure 8. A Kevlar glove partially covered with our synthetic scaled skin: Finger in the (a) extended and (b) bent position.

cotton textiles, which may be employed for transparent protective layers. We also could bond alumina scales onto carbon fibers mats, creating materials which may find applications in morphing structures that requires penetration resistance. The fabrication approach presented here is easy to implement and versatile since it can be adapted to different flexible backing layer, synthetic scales and it can be used to cover large surfaces. For example, figure 8 shows a Kevlar glove partially covered with ceramic scales which were fabricated and deposited using the stretch-and-release method. These figures demonstrate the capability of the proposed technique to cover large and complex surfaces and it demonstrates that the bio-inspired scaled skin can bend at relatively large curvatures and in two directions. We also tested the glove with a drop tower with a sharp impactor and at an impact energy of 16 mJ. A silicone tube was placed in the glove finger to simulate the presence of a finger. The bare Kevlar glove was easily punctured upon impact and did not offer any protection to the inner soft material which was perforated (see supplementary material). In contrast, the same sharp impactor dropped on the scaled glove buckled and bounced back without leaving any damage to the surface or to the inner soft material.

Acknowledgments

This work was supported by a Discovery Grant from the Natural Sciences and Engineering Research Council of Canada and by a Team Grant from the Fonds de recherche du Québec—Nature et Technologies. Certain images in this publication have been obtained by the authors from the Wikipedia/Wikimedia website, where they were made available under a Creative Commons licence or stated to be in the public domain. Please see individual figure captions in this publication for details. To the extent that the law allows, IOP Publishing disclaim any liability that any person may suffer as a result of accessing, using or forwarding the image(s). Any reuse rights should be checked and permission should be sought if necessary from

Wikipedia/Wikimedia and/or the copyright owner (as appropriate) before using or forwarding the image(s).

References

- [1] Zhu D, Ortega C F, Motamedi R, Szewciw L, Vernerey F and Barthelat F 2012 Structure and mechanical performance of a ‘Modern’ fish scale *Adv. Eng. Mater.* **14** B185–94
- [2] Bruet B J F, Song J, Boyce M C and Ortiz C 2008 Materials design principles of ancient fish armour *Nat. Mater.* **7** 748–56
- [3] Chen P-Y, Schirer J, Simpson A, Nay R, Lin Y-S, Yang W, Lopez M I, Li J, Olevsky E A and Meyers M A 2012 Predation versus protection: fish teeth and scales evaluated by nanoindentation *J. Mater. Res.* **27** 100–12
- [4] Yang W *et al* 2014 Protective role of arapaima gigas fish scales: structure and mechanical behavior *Acta Biomater.* **10** 3599–614
- [5] Dastjerdi A K and Barthelat F 2014 Teleost fish scales amongst the toughest collagenous materials *J. Mech. Behav. Biomed. Mater.* **52** 95–107
- [6] Vernerey F J and Barthelat F 2010 On the mechanics of fishscale structures *Int. J. Solids Struct.* **47** 2268–75
- [7] Rudykh S, Ortiz C and Boyce M C 2015 Flexibility and protection by design: imbricated hybrid microstructures of bio-inspired armor *Soft Matter.* **11** 2547–54
- [8] Vernerey F J and Barthelat F 2014 Skin and scales of teleost fish: simple structure but high performance and multiple functions *J. Mech. Phys. Solids* **68** 66–76
- [9] Martini R and Barthelat F 2016 Stability of hard plates on soft substrates and application to the design of bioinspired segmented armor *J. Mech. Phys. Solids* **92** 195–209
- [10] Yang W, Chen I H, Gludovatz B, Zimmermann E A, Ritchie R O and Meyers M A 2013 Natural flexible dermal armor *Adv. Mater.* **25** 31–48
- [11] Burger J and Zappalorti R T 2011 *The Northern Pine Snake (Pituophis Melanoleucus): its Life History, Behavior and Conservation* (New York: Nova Science Publishers, Inc.)
- [12] Dien A E and Brief A 2000 Survey of defensive armor across asia *J. East Asian Archaeol.* **2** 1–22
- [13] Summer G and D’Adamo R 2009 *Arms and Armour of the Imperial Roman Soldier: from Marius to Commodus* (London: Frontline Books)
- [14] Laufer B 1914 *Chinese Clay Figures: Prolegomena on the history of defensive armor: 1.* (Chicago, IL: Field Museum of Natural History)
- [15] Lee B L, Walsh T F, Won S T, Patts H M, Song J W and Mayer A H 2001 penetration failure mechanisms of armor-grade fiber composites under impact *J. Compos. Mater.* **35** 1605–33
- [16] Sloan F and Nguyen H 1995 Mechanical characterization of extended-chain polyethylene (ecpe) fiber-reinforced composites *J. Compos. Mater.* **29** 2092–107

- [17] Mayo J B, Wetzel E D, Hosur M V and Jeelani S 2009 Stab and puncture characterization of thermoplastic-impregnated aramid fabrics *Int. J. Impact Eng.* **36** 1095–105
- [18] Shin H-S, Erlich D C, Simons J W and Shockey D A 2006 Cut resistance of high-strength yarns *Text. Res. J.* **76** 607–13
- [19] Kim H and Nam I 2012 Stab resisting behavior of polymeric resin reinforced p-aramid fabrics *J. Appl. Polym. Sci.* **123** 2733–43
- [20] Decker M J, Halbach C J, Nam C H, Wagner N J and Wetzel E D 2007 Stab resistance of shear thickening fluid (STF)-treated fabrics *Compos. Sci. Technol.* **67** 565–78
- [21] Yang B, Kozey V, Adanur S and Kumar S 2000 Bending, compression, and shear behavior of woven glass fiber–epoxy composites *Compos. Part B Eng.* **31** 715–21
- [22] Neal M L 2003 Encapsulated imbricated armor system *US* 6510777B2
- [23] Chintapalli R K, Mirkhalaf M, Dastjerdi A K and Barthelat F 2014 Fabrication, testing and modeling of a new flexible armor inspired from natural fish scales and osteoderms *Bioinspir. Biomim.* **9** 036005
- [24] Ghosh R, Ebrahimi H and Vaziri A 2014 Contact kinematics of biomimetic scales *Appl. Phys. Lett.* **105** 2337011–4
- [25] Funk N, Vera M, Szewciw L J, Barthelat F, Stoykovich M P and Vernerey F J 2015 bioinspired fabrication and characterization of a synthetic fish skin for the protection of soft materials *ACS Appl. Mater. Interfaces* **7** 5972–83
- [26] Lacour S P, Jones J, Wagner S, Li T and Suo Z 2005 Stretchable interconnects for elastic electronic surfaces *Proc. IEEE* **93** 1459–66
- [27] Xu F, Lu W and Zhu Y 2011 Controlled 3D buckling of silicon nanowires for stretchable electronics *ACS Nano* **5** 672–8
- [28] Sun Y G and Rogers J A 2007 Structural forms of single crystal semiconductor nanoribbons for high-performance stretchable electronics *J. Mater. Chem.* **17** 832–40
- [29] Chai H and Lawn B R 2004 Fracture mode transitions in brittle coatings on compliant substrates as a function of thickness *J. Mater. Res.* **19** 1752–61
- [30] Rudykh S and Boyce M C 2014 Transforming small localized loading into large rotational motion in soft anisotropically structured materials *Adv. Eng. Mater.* **16** 1311–7
- [31] Zhu D, Szewciw L, Vernerey F and Barthelat F 2013 Puncture resistance of the scaled skin from striped bass: collective mechanisms and inspiration for new flexible armor designs *J. Mech. Behav. Biomed. Mater.* **24** 30–40
- [32] Ashby M F, Gibson L J, Wegst U and Olive R 1995 The mechanical properties of natural materials: I. Material property charts *Proc. R. Soc. London A* **450** 123–40